



High resolution retrieval of liquid water vertical distributions using collocated Ka-band and W-band cloud radars

Dong Huang,¹ Karen Johnson,¹ Yangang Liu,¹ and Warren Wiscombe^{1,2}

Received 14 October 2009; revised 16 November 2009; accepted 23 November 2009; published 30 December 2009.

[1] The retrieval of cloud water content using dual-frequency radar attenuation is very sensitive to error in radar reflectivity. Either a long radar dwell time or an average over many range gates is needed to reduce random noise in radar data and thus to obtain accurate retrievals – but at the cost of poorer temporal and spatial resolution. In this letter we have shown that, by using advanced mathematical inversion techniques like total variation regularization, vertically resolved liquid water content can be retrieved at an accuracy of about 0.15 gm^{-3} at 40 m resolution. This is demonstrated using the co-located Ka-band and W-band cloud radars operated by the Atmospheric Radiation Measurement program. The liquid water path calculated from the radars agrees closely with that from a microwave radiometer, with a mean difference of 70 gm^{-2} . Comparison with lidar observations reveals that the dual-frequency retrieval also reasonably captures the cloud base height of drizzling clouds – something that is very difficult to determine from radar reflectivity alone.

Citation: Huang, D., K. Johnson, Y. Liu, and W. Wiscombe (2009), High resolution retrieval of liquid water vertical distributions using collocated Ka-band and W-band cloud radars, *Geophys. Res. Lett.*, 36, L24807, doi:10.1029/2009GL041364.

1. Introduction

[2] Low and middle level stratus and stratocumulus are crucial modulators of the Earth's radiation budget because they are optically thick and cover about 46% of the globe on average [Rossow and Schiffer, 1999]. Yet, such clouds are poorly represented in numerical models and are considered as one of the largest uncertainties in predictions of climate change. Part of the reason is that existing techniques cannot provide accurate observations of clouds at the temporal and spatial resolution required for the study of radiation and cloud physical processes [Stephens, 2005].

[3] The potential of millimeter wavelength radar to observe clouds has been recognized for many years [Hobbs et al., 1985; Lhermitte, 1987; Frisch et al., 1995, 1998; Kollias et al., 2005; Matrosov, 2005]. In the Rayleigh approximation radar reflectivity is proportional to the sixth moment of cloud drop size distribution, but the sixth moment is usually not the most useful parameter for cloud microphysical and cloud radiation transfer studies. In order to obtain more useful moments like the third moment, cloud liquid water content (LWC), from radar reflectivity, certain

assumptions have to be made on the cloud drop size distribution. Natural deviations from these assumptions result in inaccurate relationships between LWC and radar reflectivity [Liu et al., 2008]. Furthermore, a small concentration of large drizzle drops can dominate the radar reflectivity yet contribute little to cloud LWC and optical depth. Unfortunately, drizzle is found to be almost ubiquitous in marine and continental stratocumulus clouds from both field campaign studies and satellite observations [Fox and Illingworth, 1997; Mace et al., 2007].

[4] The dual-frequency radar attenuation technique was therefore proposed to overcome the limitations inherent in single-frequency radar techniques to retrieve cloud LWC and effective drop size [Atlas, 1954; Eccles and Mueller, 1971; Martner et al., 1993; Vivekanandan et al., 1999; Hogan et al., 2005]. A promising property of the dual-frequency approach is that the difference in the reflectivity factors measured at two different frequencies is directly proportional to the path-integrated LWC and no assumptions on the nature of the cloud drop size distribution are needed, provided only that the cloud drops are small enough to scatter within the Rayleigh regime ($<0.5 \text{ mm}$). A further advantage is that the technique does not require absolute calibration of the individual radars; therefore only the capability of measuring the difference in radar reflectivity at two frequencies is needed.

[5] Earlier studies showed that, when 10 and 35 GHz frequencies are used, it is necessary to average over many range gates for a relatively long time period to reduce the random error in radar reflectivity and to obtain acceptable retrieval accuracy [Martner et al., 1993; Vivekanandan et al., 1999]. For example, the two-way differential attenuation of liquid water at 10 and 35 GHz is measurable only when the reflectivity factors are averaged over tens of range gates, roughly 4 km [Martner et al., 1993]. Hogan et al. [2005] suggested that using 35 and 94 GHz frequencies can substantially improve the retrieval sensitivity; under ideal conditions accurate retrieval of LWC is achievable when the precision of radar observations is reduced to 0.03 dBZ by increasing the dwell time to one minute and by averaging the data over two range gates (150 m).

[6] Theoretically, prolonged radar dwelling can only reduce the random noise in the data (thus improve the precision of radar reflectivity), but bias errors will not necessarily be damped with a longer dwell time. This poses a challenge to the dual-frequency approach since high resolution retrieval of cloud liquid water is very sensitive to both the random and non-random errors in the radar reflectivity. Advanced mathematical techniques such as total variation regularization have been widely used in solving ill-posed problems and in recovering corrupted noisy digital images. This work adopts such mathematical techniques

¹Brookhaven National Laboratory, Upton, New York, USA.

²NASA Goddard Space Flight Center, Greenbelt, Maryland, USA.

into the dual-frequency approach and examines the utility of these techniques using radar data collected by the Department of Energy Atmospheric Radiation Measurement (ARM) program.

2. Methodology

[7] The attenuated radar reflectivity factor Z_f , often expressed in conventional logarithmic unit dBZ, at frequency f and height h can be calculated from the unattenuated reflectivity factor Z^u at the same height and the one-way atmospheric attenuation coefficient α_f (dB km⁻¹). The formula can be written as [Hogan *et al.*, 2005]:

$$Z_f(h) = Z^u(h) - 2 \int_0^h \alpha_f(z) dz. \quad (1)$$

Note the unattenuated reflectivity factor Z^u is not a function of radar frequency f , provided that the radar scattering is in the Rayleigh regime. Here we assume that any difference between the dielectric factor $|K|^2$ at the frequency f and that at an unattenuated frequency is already included in the calculation of radar reflectivity factors (the ARM radar data already take this difference into account).

[8] Assuming $f = 35$ and 95 GHz respectively in equation (1), and performing a simple manipulation leads to,

$$Z_{35}(h) - Z_{95}(h) = 2 \int_0^h [\alpha_{95}(z) - \alpha_{35}(z)] dz \quad (2)$$

[9] The attenuation of radar signal is mainly due to cloud liquid water and gas absorption. The radar attenuation coefficient α_f at level h is a linear function of the mean LWC, denoted as x , at the same level,

$$\alpha_f(h) = \kappa_f(h) \cdot x(h) + \alpha^{\text{other}}(h), \quad (3)$$

where κ_f is the attenuation efficiency coefficient of liquid water (dB km⁻¹ (gm⁻³)⁻¹), and α^{other} is the attenuation by other atmospheric components (water vapor and oxygen). In the Rayleigh approximation, the formulae for calculating these attenuation coefficients for non-precipitating clouds are those of *Westwater* [1972].

[10] A numerical quadrature for equation (2) can be obtained by dividing the cloudy domain into N layers that are equally separated by distance Δh . Let h_i, h_{i+1} be the heights of the bottom and top of layer i , and x_i be the mean LWC in the layer i . Substituting equation (3) to equation (2), it is easy to show that the vertical distribution of cloud LWC is related to the difference between radar attenuation at 35 and 95 GHz:

$$\left\{ \begin{array}{l} Z_{35}(h_1) - Z_{95}(h_1) - \beta_1 = 2\Delta h(\kappa_{95} - \kappa_{35})x_1 \\ Z_{35}(h_2) - Z_{95}(h_2) - (\beta_1 + \beta_2) = 2\Delta h(\kappa_{95} - \kappa_{35})(x_1 + x_2) \\ \vdots \\ Z_{35}(h_3) - Z_{95}(h_3) - \sum_{j=1}^i \beta_j = 2\Delta h(\kappa_{95} - \kappa_{35}) \sum_{j=1}^i x_j \\ \vdots \end{array} \right. , \quad (4)$$

where $\beta_i = \Delta h[\alpha_{95}^{\text{other}}(h_i) + \alpha_{95}^{\text{other}}(h_{i-1}) - \alpha_{35}^{\text{other}}(h_i) - \alpha_{35}^{\text{other}}(h_{i-1})]$ represents the difference in radar reflectivity caused by the absorption from atmospheric absorptive components other than cloud liquid water. Since the focus of this paper is to examine the validity of the dual-frequency radar method for retrieving vertical profiles of cloud LWC, we assume the attenuation by water vapor and oxygen can be calculated exactly from nearby radiosonde ascents. Here we neglect the dependence of the absorption efficiency coefficient κ_f on height h .

[11] The system of equation (4) can be solved analytically (direct approach) given that the radar reflectivity factors can be measured at each layer at 35 and 95 GHz frequencies by a dual-frequency radar. However, many studies have shown that the direct solution is very sensitive to error in the radar reflectivity [Martner *et al.*, 1993; Hogan *et al.*, 2005]. For example, for a typical mid-latitude stratocumulus a 0.5 dBZ error in each of the 35 and 95 GHz radar reflectivities corresponds to a 2.0 gm⁻³ error in the LWC retrieval (assuming $\Delta h = 50$ m), which makes the direct approach almost useless. Here we convert the retrieval problem of dual-frequency radar into the inversion of a matrix equation (equation (5)) so that regularization techniques (constrained approaches) can be used to improve the retrieval of cloud LWC from noisy radar data.

$$\mathbf{Ax} = \mathbf{b}, \quad (5)$$

where $\mathbf{x}^T = (x_1, x_2, \dots, x_n)$ is the vector of cloud LWC; $\mathbf{b}^T = (b_1, b_2, \dots, b_n)$ is the vector of radar differential attenuation where b_i equals the left-hand side of equation (4); and $\mathbf{A} = (a_{ij})$ is a triangular matrix with its entry:

$$\alpha_{ij} = \begin{cases} 2\Delta h(\kappa_{95} - \kappa_{35}), & \text{if } i \geq j \\ 0, & \text{otherwise} \end{cases}. \quad (6)$$

[12] Equation (5) is then solved using the total variation (TV) regularization approach, a widely-used technique in image denoising applications as well as ill-posed inversion problems whose solutions are sensitive to noise. Instead of minimizing the rms difference between predictions (\mathbf{Ax}) and observations (\mathbf{b}), the constrained solution minimizes the total variation of the retrieval subject to the data constraint:

$$\min_x \{ \|\mathbf{x}\|_1 \}, \text{ subject to } \|\mathbf{Ax} - \mathbf{b}\|_2^2 \leq \varepsilon \text{ and } \mathbf{x} \geq 0. \quad (7)$$

The notations $\|\cdot\|_1$ and $\|\cdot\|_2$ stand for the L_1 and L_2 norm of a vector, and ε is an error tolerance usually set to the estimated uncertainties in the observations and in the forward model. In this study, we set the error tolerance ε to be $\sqrt{2} \times 0.5n$ dBZ, where n is the dimension of the observation vector \mathbf{b} and 0.5 dBZ represents the uncertainty in the measured radar reflectivity for both precipitation and non-precipitation range gates.

[13] Unlike the L_2 norm Tikhonov regularization that usually penalizes more the large values and thus tends to bias toward a smooth solution [Strong and Chan, 2003], the L_1 norm TV regularization does not penalize discontinuities in the solution, while simultaneously not penalizing

smoothness in the solution either; thus under certain conditions it can preserve the exact discontinuous edge in the solution [Acar and Vogel, 1994; Chambolle and Lions, 1997]. A numerical implementation of the TV regularization described by Huang *et al.* [2009] is used here to solve problem (7). This retrieval algorithm is iterative and it adaptively finds the solution that satisfies the data constraint (within the error tolerance ε) when moving towards the direction of the smallest total variation.

3. Data and Instruments

[14] The main datastreams used in this study are from the vertically-pointing millimeter wavelength cloud radar (MMCR) and W-band ARM cloud radar (WACR), both of which have been operated at ARM's Southern Great Plains (SGP) central facility for years.

3.1. Millimeter Wavelength Cloud Radar

[15] The MMCR operates at a frequency of 35 GHz (8 mm) with 0.2° beamwidth. The MMCR cycles through several distinct operating modes, each optimized for specific types and locations of clouds and precipitation [Clothiaux *et al.*, 2000]. The focus of this study is to examine the validity of the dual-frequency radar technique for retrieving cloud LWC profiles, so we use the data from only the boundary layer mode (mode 1). Under the boundary layer operating mode, the dwell and processing time is two seconds and the reflectivity measurements are accurate to within 0.5–1.0 dB with 45 m vertical resolution.

3.2. W-Band ARM Cloud Radar

[16] The 95 GHz (3.15 mm) WACR is installed in the same shelter as the 35 GHz MMCR in order to maximize overlap (a few meters separation). The beam width of the WACR is 0.35° and the vertical resolution is 43 m. The estimated uncertainty of measured reflectivity is about 0.5 dB. The WACR does not use pulse coding and alternates through the copolarization and cross-polarization modes every four seconds [Kollias *et al.*, 2005]. The data from the copolarization mode are used in this study.

3.3. Lidar Cloud Base Height

[17] The Active Remote Sensing of Clouds (ARSCL) value-added product (VAP) combines data from active remote sensors to produce an objective determination of hydrometeor height distributions [Clothiaux *et al.*, 2000]. The ARSCL cloud base height will be used in this study to evaluate the dual-frequency radar retrievals. The determination of cloud base height in the ARSCL algorithm relies on the commercial Vaisala laser ceilometer and a micropulse lidar located at the SGP facility [Clothiaux *et al.*, 2000].

3.4. Microwave Radiometer

[18] The MWR measures the downwelling microwave radiant energy of the sky (usually converted to brightness temperature for convenience) at 23.8 and 31.4 GHz frequencies. The water vapor and liquid water signals can be separated by observing at these two frequencies. The beam width is 5.5° at 23.8 GHz and is 4.6° at 31.4 GHz. The sampling time of the MWR is 20 seconds. The retrieval accuracy of the liquid water path (LWP) under low and

intermediate liquid water conditions is about 30 gm^{-2} [Turner *et al.*, 2007].

4. Retrieval Results and Error Analysis

[19] The constrained algorithm is used to retrieve cloud LWC profiles from the ARM Ka- and W-band radars at the SGP central facility, followed by an evaluation of the dual-frequency retrievals using a nearby microwave radiometer and a lidar. We present the result of May 6, 2006 here because this particular day contains clouds with very different water content and drop size.

4.1. Retrieval Results

[20] The MMCR and WACR are not ideally synchronized: their beamwidths, gate lengths and sampling rates are different. Data from both instruments must first be interpolated to a common time and space grid. We choose a temporal resolution of four seconds since this is close to the sample rate of each of the radar operating modes of interest in this study. The vertical resolution is set to 40 m. The data are then averaged to obtain a temporal resolution of 20 seconds. To remove the effects of reflectivity drift or bias, we adjust the MMCR data so that they match those of WACR at the second range gate that show a significant radar return (the first range gate may contain large interpolation error). Figure 1a depicts the 95 GHz reflectivity field between 1200 and 2400 UTC overlaid with the ARSCL cloud base height. A rain rate of 15 mm/h was recorded around 1100 UTC. From 1200 to 1700 UTC the cloud was drizzling and the corresponding radar reflectivity fields appear to be highly variable. High reflectivity factors are seen at all levels, indicating ubiquitous drizzle or rain presence.

[21] We use the temperature and pressure fields from the ARM merged sounding Value-Added Product and subtract the gaseous attenuation (water vapor and oxygen) from the radar reflectivities by using the water vapor mixing ratio calculated by assuming 100% relative humidity in clouds.

[22] The LWC field retrieved using the algorithm of equation (7) is shown in Figure 1b (referred as to constrained retrieval hereafter). Several interesting features are identifiable. A general increase in LWC with height is apparent. The majority of cloud water is located at upper cloud layers around 1100 m and 3000 m. The maximum LWC found in the cloud is about 1.5 gm^{-3} .

[23] We then compare the constrained approach with that of Hogan *et al.* [2005] (referred as to direct approach hereafter). Note that the direct approach is designed for cases with high signal-to-noise ratio, or equivalently, low resolution. The comparison is only to show the benefits of the constrained approach for high resolution retrievals. To apply the direct approach, the radar data are averaged and resampled in the same manner as described in the beginning of this section. Vertical smoothing is then performed using a moving average over five neighboring range gates (if the total number of valid gates are less than five then the window size becomes two). We also correct the reflectivity bias by subtracting the value at ARSCL cloud base from the calculated radar differential attenuation. Figure 1c shows that the direct retrieval looks noisy (for better visualization, negative values are shown in black, and values larger than

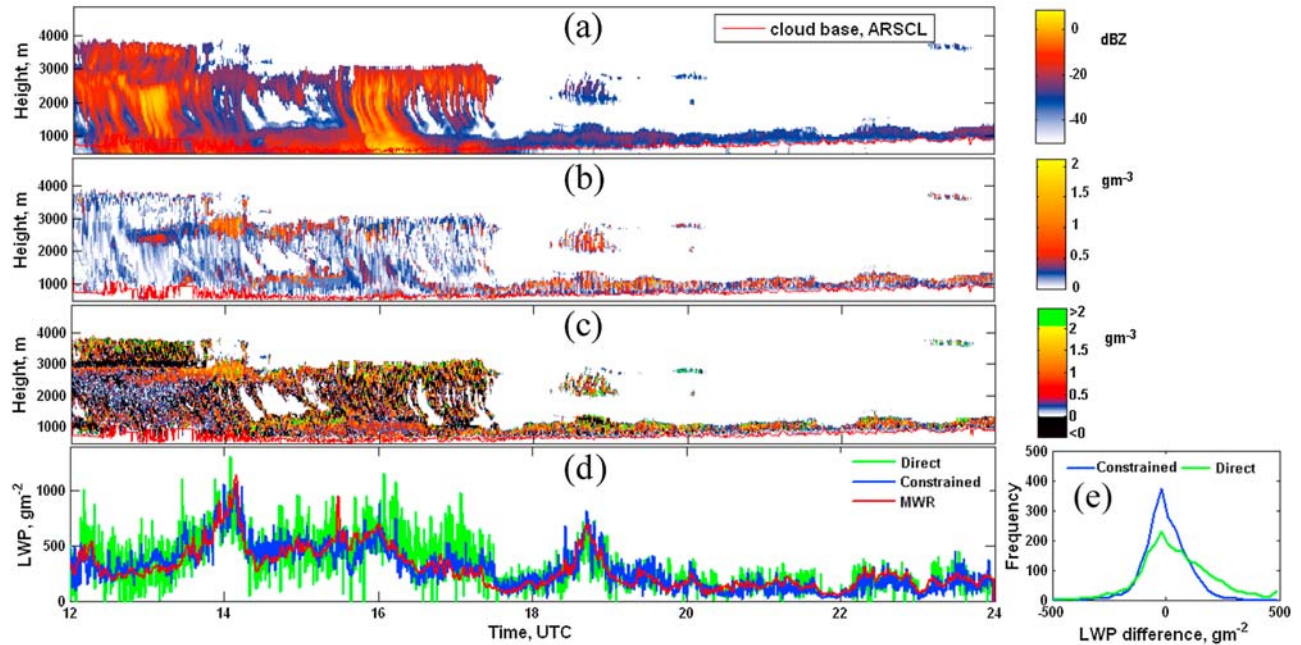


Figure 1. Dual-frequency radar observations at the Southern Great Plains central facility site on May 6, 2006: (a) radar reflectivity factor at 95 GHz by the WACR with the ARSCL lidar cloud base shown as red line; (b) the dual-frequency radar cloud LWC retrieval using the constrained approach present in this letter; (c) the retrieval using the direct approach [Hogan *et al.*, 2005]. For better visualization, negative values are shown in black, and values larger than 2.0 gm^{-3} are shown in green. Note that the direct approach is designed only for high signal-to-noise ratio cases, or equivalently, low resolution. The comparison is only to show the benefits of the constrained approach for high resolution retrievals. (d) Time series of the radar LWPs in comparison with the reference LWP from the microwave radiometer; (e) the histograms of the corresponding difference in LWP (radar LWP – MWR LWP).

2.0 gm^{-3} are shown in green). This suggests that the direct approach will need more temporal and spatial averaging in order to accumulate enough precision for practical retrieval.

[24] Figure 1d shows the temporal variation of the constrained LWP retrieval (blue), along with the MWR LWP (red). The overall agreement is good with a mean difference of 70 gm^{-2} . The dual-frequency radar LWP shows substantially more variation than the MWR LWP, since the MWR beamwidth is one order wider than the beamwidth of the radars. From 1200 to 1700 UTC, the dual-frequency LWP closely follows the trend of the MWR LWP, but appears to be systematically larger. This bias is indicative of Mie scattering effects from drizzle particles found at all range gates, and may possibly be corrected using Mie calculation and Doppler spectra. During the non-precipitating period (1700 to 2400 UTC), the dual-frequency retrieval agrees faithfully with the MWR LWP with a difference less than 30 gm^{-2} . But this agreement does not guarantee the accuracy of the vertical partition of cloud LWC. By overlaying the ARSCL cloud base with the retrieved LWC field (Figure 1b), we see that the dual-frequency retrieval not only faithfully captures the cloud base at non-drizzling regions but also reasonably identifies the cloud base at the drizzling regions. It should be emphasized that for such a drizzling case it is almost impossible to distinguish cloud base using the radar reflectivity alone and this can be easily verified in Figure 1a. Also plotted in Figure 1d is the time series of LWP from the direct retrieval (green line). The mean difference with the MWR LWP is about 120 gm^{-2} .

Figure 1e shows the histograms of the error in LWP retrievals for the two approaches.

4.2. Error Analysis

[25] The dependence of the LWC retrieval on the precision of the reflectivity measurements, on the accuracy of the temperature profile, and on the validity of the Rayleigh scattering assumption is thoroughly examined by Hogan *et al.* [2005]. We thus present only the error analysis specific to the total variation regularization algorithm in this letter.

[26] Let \mathbf{G} represents the pseudo-inverse of the regularized kernel matrix in equation (7), then the total error ϵ_x of the retrieved LWC can be written as:

$$\epsilon_x = \left[\mathbf{G} - (\mathbf{A}^T \mathbf{A})^{-1} \mathbf{A}^T \right] \mathbf{b} + \mathbf{G} \epsilon_b \quad (8)$$

where ϵ_b is the measurement error. Here we adopt the terminologies used by Rodgers [2000]. The first term on the right hand side of equation (8) is called smooth error, and it represents the way in which the regularization smooths the profile. The larger the weight carried by the regularization term, the larger the smooth error will be. The smooth error cannot be calculated exactly without knowing the true state \mathbf{x} . The second term is the error in the retrieval due to the total measurement error in radar differential attenuation. It is called retrieval error because it is due to ϵ_b , rather than the regularization. The retrieval error of the regularized solution is much smaller than that of the con-

ventional least squares solution because the small singular values in the kernel matrix are removed by regularization.

[27] Following the triangular inequality, the upper bound of the total error can be written as:

$$\|\epsilon_x\|_2 \leq \left\| \left(\mathbf{G} - (\mathbf{A}^T \mathbf{A})^{-1} \mathbf{A}^T \right) \mathbf{b} \right\|_2 + \|\mathbf{G}\epsilon_b\|_2 \quad (9)$$

The optimization algorithm used in this research chooses a weight for the regularization term in such a way that the two terms on the right hand side of equation (9) are comparable [Huang et al., 2009]. So the rms error of the retrieval can be estimated as $2\|\mathbf{G}\epsilon_b\|_2$ and thus can be calculated numerically. The retrieved LWC is estimated to be accurate to within 0.1–0.15 gm^{-3} for the cases we have tested.

5. Conclusions

[28] The dual-frequency radar approach takes advantage of the fact that the difference in radar attenuation at 35 and 95 GHz frequencies is directly proportional to the total amount of cloud LWC in the involved volume. The differential attenuation is about $7.1 \text{ dB km}^{-1} (\text{gm}^{-3})^{-1}$ under a typical environmental condition and this means that the retrieved LWC is accurate only to within 2.0 gm^{-3} assuming 50 m vertical resolution of the retrieval and 0.5 dBZ uncertainty in the radar reflectivity factors. A long radar dwell time and an average of data over many range gates are thus needed in order to improve the precision of radar observations. However this degrades the temporal and spatial resolution of the retrievals. In this paper we take a different approach – employing a constrained inversion technique, called total variation regularization. We demonstrate that the feasibility to retrieve vertically resolved cloud LWC at high temporal and spatial resolution using ARM’s co-located Ka-band and W-band cloud radars.

[29] We selected the case of May 6, 2009 to examine the validity of the dual-frequency radar technique, since this case contains very different cloud types. The retrieved cloud LWC field appears to be physically plausible. The LWPs calculated from the retrieved LWC profiles agree closely with those retrieved with the MWR, with a mean difference of 70 gm^{-2} . Despite that the beamwidths of the two radars and the microwave radiometer differ by more than 10x, the dual-frequency retrieval closely agrees with the microwave radiometer retrieval. This agreement, of course, doesn’t guarantee the validity of the retrieved LWC profiles. The validity of one aspect of the profiles, cloud base height, is clear however. The dual-frequency retrieval reasonably captures cloud base heights compared with the lidar observations, though cloud base is difficult to identify for a drizzling cloud with radar reflectivity alone. Further validation of the dual-frequency radar retrieval requires concurrent independent observations of cloud water profile either by in-situ airborne cloud sensors or by a network of surface-based microwave radiometers using the cloud tomography approach [Huang et al., 2008].

[30] **Acknowledgments.** This work is supported by the DOE Atmosphere Radiation Measurement program under contract DE-AC02-98CH10886. We thank Robin Hogan, Pavlos Kollias, and Michael Jensen

for insightful discussions. We are grateful to Virendra Ghate for providing the non-precipitating cloud cases.

References

- Acar, R., and C. Vogel (1994), Analysis of total variation penalty methods, *Inverse Probl.*, *10*, 1217–1229, doi:10.1088/0266-5611/10/6/003.
- Atlas, D. (1954), The estimation of cloud parameters by radar, *J. Meteorol.*, *11*, 309–317.
- Chambolle, A., and P. Lions (1997), Image recovery via total variation minimization and related problems, *Numer. Math.*, *76*, 167–188, doi:10.1007/s002110050258.
- Clothiaux, E., T. Ackerman, G. Mace, K. Moran, R. Marchand, M. Miller, and B. Martner (2000), Objective determination of cloud heights and radar reflectivities using a combination of active remote sensors at the ARM CART sites, *J. Appl. Meteorol.*, *39*, 645–665, doi:10.1175/1520-0450(2000)039<0645:ODOCHA>2.0.CO;2.
- Eccles, P., and E. Mueller (1971), X-band attenuation and liquid water content estimation by dual-wavelength radar, *J. Appl. Meteorol.*, *10*, 1252–1259, doi:10.1175/1520-0450(1971)010<1252:XBAALW>2.0.CO;2.
- Fox, N., and A. Illingworth (1997), The potential of a spaceborne radar for the detection of stratocumulus clouds, *J. Appl. Meteorol.*, *36*, 676–687, doi:10.1175/1520-0450(1997)036<0485:TROSCP>2.0.CO;2.
- Frisch, A. S., C. W. Fairall, and J. B. Snider (1995), Measurement of stratus cloud and drizzle parameters in ASTEX with a Ka-band Doppler radar and a microwave radiometer, *J. Atmos. Sci.*, *52*, 2788–2799, doi:10.1175/1520-0469(1995)052<2788:MOSCAD>2.0.CO;2.
- Frisch, A. S., G. Feingold, C. W. Fairall, T. Uttal, and J. B. Snider (1998), On cloud radar and microwave radiometer measurements of stratus cloud liquid water profiles, *J. Geophys. Res.*, *103*, 23,195–23,197, doi:10.1029/98JD01827.
- Hobbs, P., N. Funk, R. Weiss Sr., J. Locatelli, and K. Biswas (1985), Evaluation of a 35 GHz radar for cloud physics research, *J. Atmos. Oceanic Technol.*, *2*, 35–48, doi:10.1175/1520-0426(1985)002<0035:EOAGRF>2.0.CO;2.
- Hogan, R., N. Gaussiat, and A. Illingworth (2005), Stratocumulus liquid water content from dual-wavelength radar, *J. Atmos. Oceanic Technol.*, *22*, 1207–1218, doi:10.1175/JTECH1768.1.
- Huang, D., Y. Liu, and W. Wiscombe (2008), Determination of cloud liquid water distribution using 3D cloud tomography, *J. Geophys. Res.*, *113*, D13201, doi:10.1029/2007JD009133.
- Huang, D., A. Gasiewski, and W. Wiscombe (2009), Retrieval of cloud liquid water distributions from a single scanning microwave radiometer aboard a moving platform. Part I: Field trial results from the Wakasa Bay experiment, *Atmos. Chem. Phys. Discuss.*, *9*, 12,027–12,064.
- Kollias, P., B. Albrecht, E. Clothiaux, M. Miller, K. Johnson, and K. Moran (2005), The atmospheric radiation measurement program cloud profiling radars: An evaluation of signal processing and sampling strategies, *J. Atmos. Oceanic Technol.*, *22*, 930–948, doi:10.1175/JTECH1749.1.
- Lhermitte, R. (1987), A 94 GHz Doppler radar for clouds observations, *J. Atmos. Oceanic Technol.*, *4*, 36–48, doi:10.1175/1520-0426(1987)004<0036:AGDRFC>2.0.CO;2.
- Liu, Y., B. Geerts, M. Miller, P. Daum, and R. McGraw (2008), Threshold radar reflectivity for drizzling clouds, *Geophys. Res. Lett.*, *35*, L03807, doi:10.1029/2007GL031201.
- Mace, G., R. Marchand, Q. Zhang, and G. Stephens (2007), Global hydro-meteor occurrence as observed by CloudSat: Initial observations from summer 2006, *Geophys. Res. Lett.*, *34*, L09808, doi:10.1029/2006GL029017.
- Martner, B., R. Kropfli, L. Ash, and J. Snider (1993), Dual-wavelength differential attenuation radar measurements of cloud liquid water content, paper presented at the 26th Conference on Radar Meteorology, Am. Meteorol. Soc., Norman, Okla.
- Matrosov, S. (2005), Attenuation-based estimates of rainfall rates aloft with vertically pointing Ka-band radars, *J. Atmos. Oceanic Technol.*, *22*, 43–54, doi:10.1175/JTECH-1677.1.
- Rodgers, C. D. (2000), *Inverse Methods for Atmospheric Sounding: Theory and Practice*, 200 pp., World Sci., Singapore.
- Rossow, W., and R. Schiffer (1999), Advances in understanding clouds from ISCCP, *Bull. Am. Meteorol. Soc.*, *80*, 2261–2287, doi:10.1175/1520-0477(1999)080<2261:AIUCFI>2.0.CO;2.
- Stephens, G. L. (2005), Cloud feedbacks in the climate system: A critical review, *J. Clim.*, *18*, 237–273, doi:10.1175/JCLI-3243.1.
- Strong, D., and T. Chan (2003), Edge-preserving and scale-dependent properties of the total variation regularization, *Inverse Probl.*, *19*, S165–S187, doi:10.1088/0266-5611/19/6/059.
- Turner, D., S. Clough, J. Liljegren, E. Clothiaux, K. Cady-Pereira, and K. Gaustad (2007), Retrieving liquid water path and precipitable water vapor from Atmospheric Radiation Measurement (ARM) microwave

- radiometers, *IEEE Trans. Geosci. Remote Sens.*, 45, 3680–3690, doi:10.1109/TGRS.2007.903703.
- Vivekanandan, J., B. Martner, M. Politovich, and G. Zhang (1999), Retrieval of atmospheric liquid and ice characteristics using dual-wavelength radar observations, *IEEE Trans. Geosci. Remote Sens.*, 37, 2325–2334, doi:10.1109/36.789629.
- Westwater, E. (1972), Microwave emission from clouds, *NOAA Tech. Rep. ERL 219-WPL 18*, 43 pp., NOAA, Silver Spring, Md.
-
- D. Huang, K. Johnson, and Y. Liu, Brookhaven National Laboratory, 75 Rutherford Dr., Upton, NY 11973, USA. (dhuang@bnl.gov)
W. Wiscombe, NASA Goddard Space Flight Center, Code 913, Greenbelt, MD 20771, USA.